Pis'ma v ZhETF, vol. 90, iss. 8, pp. 639 – 643

Topological invariant for superfluid ^{3}He-B and quantum phase transitions

G. E. Volovik[1)]

Low Temperature Laboratory, Helsinki University of Technology, FIN-02015 HUT, Finland

Landau Institute for Theoretical Physics RAS, 119334 Moscow, Russia

Submitted 22 September 2009

We consider topological invariant describing the vacuum states of superfluid ^{3}He-B, which belongs to the special class of time-reversal invariant topological insulators and superfluids. Discrete symmetries important for classification of the topologically distinct vacuum states are discussed. One of them leads to the additional subclasses of ^{3}He-B states and is responsible for the finite density of states of Majorana fermions living at some interfaces between the bulk states. Integer valued topological invariant is expressed in terms of the Green's function, which allows us to consider systems with interaction.

PACS: 71.23.An

1. Introduction. General classification schemes based on topology [1 – 7] suggest existence of the topological insulators and fully gapped topological superfluids/superconductors which have the gapless edge states on the boundary or at the interface. Superfluid ^{3}He-B belongs to the special class of three-dimensional topological superfluids with time-reversal symmetry. Topological invariant which describes the ground states (vacua) of ^{3}He-B has been discussed in Refs. [1, 8]. Here we present the explicit expression for the relevant topological invariant, and discuss topological quantum phase transitions occurring between the vacuum states and fermion zero modes living at the interfaces between the bulk states.

2. Topological invariant protected by symmetry. Usually in the topological classification of ground states people use the Hamiltonian of free particles or the corresponding effective Hamiltonian such as Dirac and Bogoliubov-de Gennes Hamiltonians [1 – 4]. However, in this classification the natural problem arises, what is the effect of interaction between particles. Moreover, the original first-principle many-body Hamiltonian of, say, liquid ^{3}He

$$\mathcal{H} - \mu\mathcal{N} = \int d\mathbf{x}\psi^\dagger(\mathbf{x})\left[-\frac{\nabla^2}{2m} - \mu\right]\psi(\mathbf{x}) + \\ + \frac{1}{2}\int d\mathbf{x}d\mathbf{y}U(\mathbf{x}-\mathbf{y})\psi^\dagger(\mathbf{x})\psi^\dagger(\mathbf{y})\psi(\mathbf{y})\psi(\mathbf{x}), \qquad (1)$$

has no information on the topological structure of the ground state of the system – superfluid ^{3}He-B. The accurate procedure to reduce such a strongly interacting many-body system to the effective coarse-grained Hamiltonian is absent. However, the microscopic Hamiltonian allows us at list in principle to calculate the Green's function $G(\omega, \mathbf{p})$ – the quantity which determines the main properties of the translational invariant or periodic ground states of the system. That is why the object for the topological classification must be the Green's function rather than Hamiltonian. Then it is applicable even in cases when one cannot introduce the effective low energy Hamiltonian, for example when Green's function does not have poles, see [6, 9].

Green's function topology has been used in particular for classification of topologically protected nodes in the quasiparticle energy spectrum of systems of different dimensions; for the classification of the topological ground states in the fully gapped $2+1$ systems, which experience intrinsic quantum Hall and spin-Hall effects [10 – 12, 5, 6, 13], including multi-band topological insulators [14]; in relativistic quantum field theory of $2+1$ massive Dirac fermions [16 – 18; etc.

The integer-valued topological invariants were expressed via the Green's function, which was considered at imaginary frequency to avoid the zeroes, poles or other possible singularities on the mass shell. In the fully gapped systems one may consider the Green's function not only at imaginary frequency, but also at real frequency if it is below the gap. For the classification of the ^{3}He-B states we shall use the Green's function at zero frequency: $\mathcal{G}(\mathbf{p}) \equiv G(\omega = 0, \mathbf{p})$. The typical example of the integer valued topological invariant is the following 3-form:

$$N = \frac{e_{ijk}}{24\pi^2}\mathbf{tr}\left[\int d^3p\mathcal{G}\partial_{p_i}\mathcal{G}^{-1}\mathcal{G}\partial_{p_j}\mathcal{G}^{-1}\mathcal{G}\partial_{p_k}\mathcal{G}^{-1}\right], \qquad (2)$$

[1)] e-mail: volovik@boojum.hut.fi

where integration is over the whole momentum space for translational invariant systems, or over the Brillouin zone in crystals. For ^{3}He-B obeying time-reversal symmetry this invariant is identically zero, $N = 0$. However, the discrete symmetries of ^{3}He-B give rise to the other invariants. Examples of additional integer valued topological invariants which appear due to symmetry in different condensed matter systems and in quantum field theory can be found in Refs. [10, 19, 12, 5, 6].

Due to symmetry, one or several Pauli matrices γ of spin, pseudospin or Bogoliubov-Nambu spin may either commute or anti-commute with the Green's function matrix:

$$\gamma \mathcal{G}(\mathbf{p}) = -\mathcal{G}(\mathbf{p})\gamma, \tag{3}$$

or

$$\gamma \mathcal{G}(\mathbf{p}) = \mathcal{G}(\mathbf{p})\gamma. \tag{4}$$

This leads to the following integer valued topological invariants:

$$N_\gamma = \frac{e_{ijk}}{24\pi^2}\mathbf{tr}\left[\gamma \int d^3p \mathcal{G}\partial_{p_i}\mathcal{G}^{-1}\mathcal{G}\partial_{p_j}\mathcal{G}^{-1}\mathcal{G}\partial_{p_k}\mathcal{G}^{-1}\right], \tag{5}$$

with $\mathcal{G}(\mathbf{p})$ and γ obeying either (3) or (4).

The topological classes of the ^{3}He-B states can be represented by the following Green's function, which plays the role of effective Hamiltonian:

$$\mathcal{G}^{-1}(\mathbf{p}) = M(p)\tau_3 + \tau_1\left(\sigma_x c_x p_x + \sigma_y c_y p_y + \sigma_z c_z p_z\right), \tag{6}$$

$$M(p) = \frac{p^2}{2m^*} - \mu, \tag{7}$$

where τ_i are Pauli matrices of Bogolyubov-Nambu spin. The overall 'conformal' factor, which may depend on $\mathbf{p}$, is omitted since it does not influence the topological invariant. In the isotropic ^{3}He-B all 'speeds of light' are equal, $|c_x| = |c_y| = |c_z| = c$. The topological invariant relevant for ^{3}He-B is N_γ in (5) with $\gamma = \tau_2$:

$$N_\gamma = \frac{e_{ijk}}{24\pi^2}\ \mathbf{tr}\left[\tau_2 \int d^3p\ \mathcal{G}\partial_{p_i}\mathcal{G}^{-1}\mathcal{G}\partial_{p_j}\mathcal{G}^{-1}\mathcal{G}\partial_{p_k}\mathcal{G}^{-1}\right]. \tag{8}$$

The τ_2 matrix plays the role of the γ-matrix, which anticommutes with the Green's function in (3). The τ_2 symmetry is combination of time reversal and particle-hole symmetries in ^{3}He-B.

3. Phase diagram in mass plane. Fig.1 shows the phase diagram of topological states of ^{3}He-B in the plane $(\mu, 1/m^*)$. On the line $1/m^* = 0$ one obtains Dirac fermions with mass parameter $M = -\mu$:

$$\mathcal{G}^{-1}(\mathbf{p}) = M\tau_3 + \tau_1\left(\sigma_x c_x p_x + \sigma_y c_y p_y + \sigma_z c_z p_z\right). \tag{9}$$

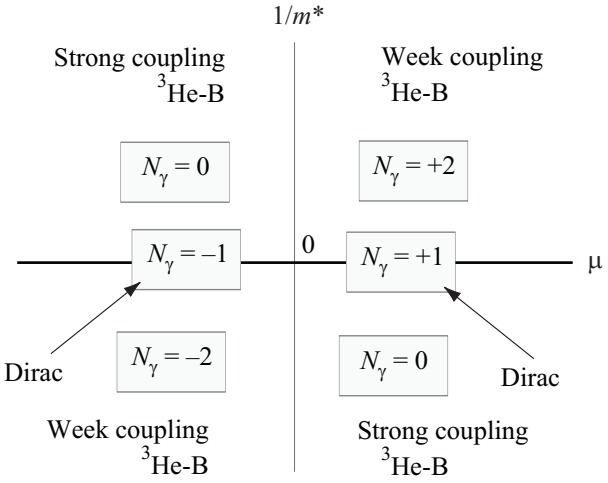

Fig.1. Phase diagram of topological states of ^{3}He-B in equation (6) in the plane $(\mu, 1/m^*)$ for the speeds of light $c_x > 0$, $c_y > 0$ and $c_z > 0$. States on the line $1/m^* = 0$ correspond to the Dirac vacua, which Hamiltonian is non-compact. Topological charge of the Dirac fermions is intermediate between charges of compact ^{3}He-B states. The line $1/m^* = 0$ separates the states with different asymptotic behavior of the Hamiltonian at infinity: $\mathcal{G}^{-1}(\mathbf{p}) \to \pm\tau_3 p^2/2m^*$. The line $\mu = 0$ marks topological quantum phase transition, which occurs between the weak coupling ^{3}He-B (with $\mu > 0$, $m^* > 0$ and topological charge $N_\gamma = 2$) and the strong coupling ^{3}He-B (with $\mu < 0$, $m^* > 0$ and $N_\gamma = 0$). This transition is topologically equivalent to quantum phase transition between Dirac vacua with opposite mass parameter $M = \pm|\mu|$, which occurs when μ crosses zero along the line $1/m^* = 0$. The interface which separates two states contains single Majorana fermion in case of ^{3}He-B, and single chiral fermion in case of relativistic quantum fields. Difference in the nature of the fermions is that in Bogoliubov-de Gennes system the components of spinor are related by complex conjugation. This reduces the number of degrees of freedom compared to Dirac case

Topological invariant (8) for Dirac fermions is

$$N_\gamma = -\mathrm{sign}(M c_x c_y c_z) = \mathrm{sign}(\mu c_x c_y c_z). \tag{10}$$

In relativistic quantum field theory, τ_2 matrix in (8) is the operator of CT symmetry [20]. Hamiltonian for Dirac fermions is non-compact, with different asymptotes at $p \to \infty$ for different directions of momentum $\mathbf{p}$. As a result, the topological charge of the Dirac fermions is intermediate between charges of the compact states of ^{3}He-B below and above the horizontal axis (see Refs. [21, 1, 5] on the marginal behavior of fermions with relativistic spectrum; also note that the topological invariant N_γ in (8) has values twice larger than the invariants introduced in Refs. [3, 8]). When the line

$1/m^* = 0$ is crossed, the asymptotic behavior of the ^{3}He-B Green's function changes from $\mathcal{G}^{-1}(\mathbf{p}) \to +\tau_3 p^2/2m^*$ to $\mathcal{G}^{-1}(\mathbf{p}) \to -\tau_3 p^2/2m^*$.

The real superfluid ^{3}He-B lives on the weak coupling side of the phase diagram: at $\mu > 0$, $m^* > 0$, $\mu \gg m^* c^2$. However, in the ultracold Fermi gases with triplet pairing the strong coupling limit is possible near the Feshbach resonance [22]. When μ crosses zero the topological quantum phase transition occurs, at which the topological charge N_γ changes from $N_\gamma = 2$ to $N_\gamma = 0$. Previously the topological quantum phase transition occurring at $\mu = 0$ has been considered for the chiral p-wave states of the ^{3}He-A type: the transition from the gapless state at $\mu > 0$ to the fully gapped state at $\mu < 0$ [19, 22]. In the ^{3}He-B case, both states are fully gapped, while the intermediate state at $\mu = 0$ is gapless: it has two point nodes at $\mathbf{p} = 0$ with opposite chiralities. There is a general relation between topological invariants of the two states and the number of point nodes in the intermediate gapless state [5], which for a given case reads:

$$N_{\text{point nodes}} = |N_\gamma(\mu > 0) - N_\gamma(\mu < 0)| = 2. \qquad (11)$$

This relation also determines the number of $2+1$ fermion zero modes living at the interface between the two states:

$$N_{\text{FZM}} = \frac{1}{2}\,|N_\gamma(\mu > 0) - N_\gamma(\mu < 0)| = 1. \qquad (12)$$

This analog of the index theorem [23] implies that such interface contains single Majorana fermion.

The same quantum phase transition occurs when μ crosses zero along the line $1/m* = 0$, i.e. the line of the relativistic Dirac fermions. At this transition the mass $M = -\mu$ of Dirac fermions changes sign. The rules (11) and (12) are also applicable for the Dirac fermions. However, in relativistic quantum field theory the domain wall separating vacua with opposite M contains chiral fermion rather than the Majorana one. Difference in the nature of the fermions comes from the observation that in the Bogoliubov-de Gennes system the components of a spinor are related by complex conjugation. This reduces the number of fermionic degrees of freedom compared to the relativistic quantum field theory and makes them the Majorana fermions.

The spectrum of fermion zero modes at this interface can be easily found in the limit $|\mu| \ll m^* c^2$, when the p^2 term in the Hamiltonian can be neglected and the Hamiltonian approaches the Dirac one. In this limit Majorana fermions in ^{3}He-B have relativistic spectrum:

$$H_{\text{zm}} = c\hat{\mathbf{z}} \cdot (\boldsymbol{\sigma} \times \mathbf{p}). \qquad (13)$$

The same spectrum is obtained for the chiral fermions living on the interface between the states of the 3D topological insulator with normal and inverted arrangements of two bands, see Ref. [24].

The invariant (8) is applicable to the general case of systems with Green's function of the type

$$\mathcal{G}^{-1}(\mathbf{p}) = \hat{\epsilon}(\mathbf{p})\tau_3 + \hat{\Delta}(\mathbf{p})\tau_1, \qquad (14)$$

where $\hat{\epsilon}$ and $\hat{\Delta}$ are Hermitian matrices with spin and band indices. This includes in particular the Hamiltonians discussed in Refs. [3, 25]. The phase diagram of topological 3D states in [3] is similar to that in Fig.1 (note again that the topological invariant N_γ has values twice larger than invariants introduced in Refs. [3, 8]).

4. Phase diagram in the speed of light plane. Fig.2 shows phase diagram of topological states of ^{3}He-B

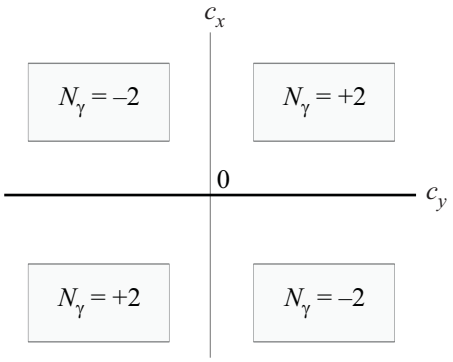

Fig.2. Phase diagram of ^{3}He-B states at fixed $c_z > 0$, $\mu > 0$ and $m^* > 0$. The interface between the states with different winding number N_γ contains Majorana fermions. However, in the presence of discrete symmetry Z_2 – combined rotation by π about z axis in spin and orbital spaces – the ^{3}He-B states with the same topological invariant N_γ may be connected only via the gapless state. As a result, the interface between two states with the same N_γ also contains Majorana fermions. These fermions have finite density of states at zero energy [8]. This is the origin of the finite density of states of the Majorana edge states on the diffusive wall [27]

in the plane (c_x, c_y) at fixed $c_z > 0$, $\mu > 0$ and $m^* > 0$. When one of the components of speed of light, say, c_x crosses zero, two pairs of point nodes appear in the intermediate gapless state, at points $\mathbf{p} = \pm(0, 0, p_F)$, where $p_F^2 = 2\mu m^*$ is Fermi momentum. This is the consequence of different topological invariant N_γ of the two states:

$$N_{\text{point nodes}} = |N_\gamma(c_x > 0) - N_\gamma(c_x < 0)| = 4. \qquad (15)$$

The intermediate state is the so called planar state [26], and the corresponding gapless fermions in this state are characterized by the topological invariant protected by discrete symmetry in (4) $\gamma = \tau_3\sigma_x$, which commutes

with Hamiltonian: $\gamma\mathcal{G}(\mathbf{p}) = \mathcal{G}(\mathbf{p})\gamma$ (see Eq.(14.4) of Ref. [5]):

$$N_3 = \frac{e_{\mu\nu\lambda\gamma}}{24\pi^2}\mathbf{tr}\left[\tau_3\sigma_x \int dS^\gamma G\partial_{p_\mu}G^{-1}G\partial_{p_\nu}G^{-1}G\partial_{p_\lambda}G^{-1}\right], \quad (16)$$

where integral is around a nodal point $p_\mu = (0, 0, p_F, 0)$ or $p_\mu = (0, 0, -p_F, 0)$ in the 4D momentum-frequency space $p_\mu = (\mathbf{p}, \omega)$. Number of Majorana fermion zero modes living at the interface between the two states is correspondingly twice smaller: $N_{\rm FZM} = 2$. The same number of $2 + 1$ fermions live at the boundary of ^{3}He-B with specular reflection. This is because there is an exact mapping between the edge states on the ^{3}He-B boundary with perfect reflection and fermion zero modes living at the interface, see Ref. [27].

There are subclasses of ^{3}He-B states, which exist due to discrete symmetry. When two components of speed of light, say, c_x and c_y cross zero, the topological charge N_γ does not change. The final state can be continuously connected with original state by spin rotation by angle π about axis z. However, there is additional discrete symmetry – the combined rotation by π about z axis in spin and orbital spaces. If this Z_2 symmetry is maintained, the two states with the same topological invariant N_γ cannot be connected by adiabatic deformations. The intermediate gapless states necessarily contains the line of nodes.

As a result the interface between states with the same N_γ, at which two components of speed of light in (10) change sign, also contains zero modes. Spectrum of these fermions $H_{\rm zm} \propto c\sigma_x k_y$, and they have finite density of states at zero energy [8, 27]. Because of the mapping between the fermion zero modes living at this interface and the edge state of ^{3}He-B on diffusive boundary, the Majorana states on the diffusive wall also have finite density of states [27] in agreement with the detailed quasiclassical theory [28].

5. Discussion. There are many experimental evidences for the Andreev surface states on the wall of ^{3}He-B, see e.g. [29 – 32], and some other experiments are proposed [33]. At low temperature, where thermal quasparticles in bulk ^{3}He-B are frozen out exponentially, the low-energy surface states – Majorana fermions – will give the main contribution to thermodynamics and dissipation, with the power-law dependence of the physical quantities. The extra discrete symmetry of ^{3}He-B essentially enhances the effect of Andreev-Majorana states by providing the finite density of states of these modes on rough walls [34]. Systems with highly developed surfaces, such as ^{3}He-B confined in porous materials, or systems of parallel plates or tubes, would be more advantageous for the direct identification of the Majorana fermions in superfluid ^{3}He-B.

It is a pleasure to thank A. Kitaev and Yu. Makhlin for valuable discussions. This work is supported in part by the Academy of Finland, Centers of Excellence Program 2006–2011, the Russian Foundation for Basic Research (grant # 06-02-16002-a), and the Khalatnikov–Starobinsky leading scientific school (grant 4899.2008.2).

1. A. P. Schnyder, S. Ryu, A. Furusaki, and A.W.W. Ludwig, Phys. Rev. B **78**, 195125 (2008).
2. A. P. Schnyder, S. Ryu, A. Furusaki, and A. W. W. Ludwig, AIP Conf. Proc. **1134**, 10 (2009); arXiv:0905.2029.
3. A. P. Schnyder, S. Ryu, and A. W. W. Ludwig, Phys. Rev. Lett. **102**, 196804 (2009); arXiv:0901.1343.
4. A. Kitaev, AIP Conf. Proc., Volume **1134**, 22 (2009); arXiv:0901.2686.
5. G. E. Volovik, *The Universe in a Helium Droplet*, Clarendon Press, Oxford, 2003.
6. G. E. Volovik, *Quantum Analogues: From Phase Transitions to Black Holes and Cosmology*, Eds. W. G. Unruh and R. Schützhold, Springer Lecture Notes in Physics **718** (2007), pp. 31–73; cond-mat/0601372.
7. P. Hořava, Phys. Rev. Lett. **95**, 016405 (2005).
8. M. M. Salomaa and G. E. Volovik, Phys. Rev. B **37**, 9298 (1988).
9. B. Farid and A. M. Tsvelik, arXiv:0909.2886.
10. G. E. Volovik and V. M. Yakovenko, J. Phys.: Condens. Matter **1**, 5263 (1989).
11. V. M. Yakovenko, Fizika (Zagreb) **21**, suppl. 3, 231 (1089); arXiv:cond-mat/9703195.
12. K. Sengupta and V. M. Yakovenko, Phys. Rev. B **62**, 4586 (2000).
13. N. Read and D. Green, Phys. Rev. B **61**, 10267 (2000).
14. G. E. Volovik, JETP **67**, 1804 (1988); in Sec. 3 the quantum Hall effect in the absence of external magnetic field is discussed for the model of two-band insulator considered in Ref. [15].
15. B. A. Volkov, A. A. Gorbatsevich, Yu. V. Kopaev, and V. V. Tugushev, JETP **54**, 391 (1981).
16. K. Ishikawa and T. Matsuyama, Z. Phys. C **33**, 41 (1986).
17. K. Ishikawa and T. Matsuyama, Nucl. Phys. B **280**, 523 (1987).
18. K. Jansen, Phys. Rept. **273**, 1 (1996).
19. G.E. Volovik, *Exotic properties of superfluid ^{3}He*, World Scientific, Singapore, 1992.
20. S. Weinberg, *The Quantum Theory of Fields*, Cambridge University Press, 1995.
21. F. D. M. Haldane, Phys. Rev. Lett. **61**, 2015 (1988).
22. V. Gurarie and L. Radzihovsky, Ann. Phys. **322**, 2 (2007).
23. R. Jackiw and P. Rossi, Nucl. Phys. B **190**, 681 (1981).

24. B. A. Volkov and O. A. Pankratov, JETP Lett. **42**, 178 (1985).
25. M. Sato, Phys. Rev. B **79**, 214526 (2009).
26. D. Vollhardt and O. Wölfle, *The superfluid phases of helium 3*, Taylor and Francis, London, 1990.
27. G. E. Volovik, Pis'ma v ZhETF **90**, 440 (2009); arXiv:0907.5389.
28. N. B. Kopnin, P. I. Soininen, and M. M. Salomaa, J. Low Temp. Phys. **85**, 267 (1991).
29. C. A. M. Castelijns, K. F. Coates, A. M. Guénault et al., Phys. Rev. Lett. **56**, 69 (1986).
30. J. P. Davis, J. Pollanen, H. Choi et al., Phys. Rev. Lett. **101**, 085301 (2008).
31. K. Nagai, Y. Nagato, M. Yamamoto, and S. Higashitani, J. Phys. Soc. Jap. **77**, 111003 (2008).
32. S. Murakawa, Y. Wada, Y. Tamura et al., J. Physics: Conf. Series **150**, 032070 (2009).
33. Suk Bum Chung and Shou-Cheng Zhang, arXiv:0907.4394.
34. Recent experiments in ^{3}He-B demonstrate that the density of surface states is suppressed if the container walls are coated by ^{4}He atoms [35]. This allows the systematic study of the Andreev-Majorana states with controllable change of boundary conditions.
35. S. Murakawa, Y. Tamura, Y. Wada et al., Phys. Rev. Lett. **103**, 155301 (2009).